

Dissolution of Biogenic Silica (bSiO₂) of Southern Ocean Diatoms at Low Temperatures

M. A. French (1, 2), M. Robert (2), A. Terbrueggen (2), T.D. Jickells (1), U. Passow (2)

(1) University of East Anglia, Norwich, UK, (2) Alfred-Wegener-Institut für Polar und Meeresforschung, Bremerhaven, Germany (meyhey@tinyworld.co.uk)

Introduction

The bSiO₂ ooze of the Southern Ocean (S.O) has long provided a source of discussion over how and why such thick accumulations exist underlying a region of relatively low diatom productivity. The low temperatures and high nutrient conditions of many regions of the S.O are understood to be optimal for *Fragilariopsis kerguelensis*, a slow growing diatom with a high silicate (Si), yet low iron requirement¹, thus making it a dominant species in the surface ocean of this region. The high level of silicification and robust characteristics of *F.kerguelensis* has been hypothesised as being a main factor contributing to its persistence in the sediments of the S.O². However, specific dissolution characteristics of this species have not previously been elucidated, nor have the effects that temperature and aggregation might have in determining the diatom composition of deep ocean sediments.

Table 1 Summary of experimental set-up

Diatom species and physiological state	Number of rolling tanks	Tank volume (l)	Incubation temperature (°C)	Duration (days) with dissolution rate period in brackets
▲ <i>Fragilariopsis kerguelensis</i> senescent cells (<i>F.kerguelensis</i>)	6	0.18	5	123 (123)
■ <i>Chaetoceros debilis</i> senescent cells (<i>C.debilis</i> ^{sen})	10	0.18	5	123 (113)
◆ <i>Chaetoceros debilis</i> senescent cells (<i>C.debilis</i> ^{sen})	12	0.18	15	122 (20; 46)
● <i>Chaetoceros debilis</i> exponentially grown cells (<i>C.debilis</i> ^{exp})	6	4	5	90 (77)

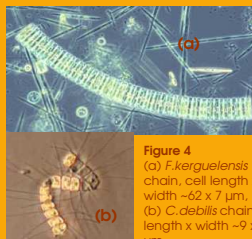


Figure 4
(a) *F.kerguelensis* chain, cell length x width -62 x 7 µm, (b) *C.debilis* chain, cell length x width -9 x 8 µm (courtesy P.Assmy).

Conclusions

- Si-Dissolution rates of the Antarctic diatom *F. kerguelensis* are at least half the rate of Antarctic *C.debilis*, which provides a possible explanation for the selective enrichment of *F. kerguelensis* in S.O sediments;
- Potential implications for Si Fluxes to the sediments can be approximated by assuming a depth of 4000 m and sinking velocities of 50 m d⁻¹ for the 'fluffy' aggregates we observe for *C.debilis* and 200 m d⁻¹ for the dense aggregates formed by *F. kerguelensis*; translating to ~97% of bSiO₂ of *F. kerguelensis* reaching sediments (after 20 days) in comparison to just ~26% of *C.debilis* (after 80 days);
- Si dissolution rates of *C.debilis* at 5°C are nearly three times that at 15°C, highlighting how low temperatures in the S.O have a diminishing effect for the dissolution of diatom frustules;
- Si dissolution rates of *C.debilis* collected from exponentially growing cells are almost zero for the 10 days, thereafter dissolution rates are similar to those of senescent cells, emphasising that opal dissolution starts only after cell death.

Methods

Batch cultures of S.O strains of *F.kerguelensis* and *Chaetoceros debilis*, grown over ~5 months to senescence (^{sen}) and *C.debilis* grown exponentially (^{exp}) over ~2 weeks, were mixed with Si-free copepod detritus and Si-free artificial seawater (ASW) then transferred to rolling tanks. Tanks were incubated at either 5 or 15°C (Fig.1) and sampled for dissolved silica (DSi) and bSiO₂ at time intervals over a ~4 month period as summarised in Table 1.



Figure 1 Rolling tank set-up



Figure 5 Aggregated *C.debilis*^{exp}

Discussion

Temperature effect

• Much of the global sedimentary bSiO₂ occurs in cold regions of the ocean³. Indeed, a lower of temperature has been shown to reduce the dissolution of cleaned diatom frustules⁴ and dissolution rate coefficients have been shown to increase by a factor of ~2 for each 10°C rise in temperature⁵.

• We show a similar effect for frustules of live aggregated *C.debilis*, whereby the averaged dissolution rate nearly trebled with a 10°C increase in temperature from 1.32 µM Si d⁻¹ (113 days) at 5°C (■) to 3.76 µM Si d⁻¹ (46 days) at 15°C (◆) (Fig.2a,b). The latter can be separated into two main stages of dissolution; an initially rapid stage between days 1 - 20 (6.96 µM Si d⁻¹) and a significantly slower stage between days 20 - 46 (0.97 µM Si d⁻¹) (Fig.2a).

• Further substantiated by the fact that virtually all *C.debilis* material rolling at 15°C (◆) dissolved after ~7 weeks (95%, Fig.3c) in comparison to 74.3% of that at 5°C (■) (Fig.3b).

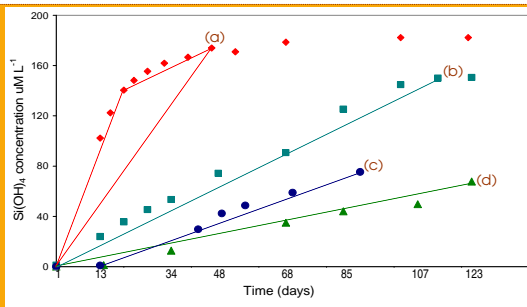


Figure 2 Dissolved silica (DSi, as Si(OH)₄ µM l⁻¹) concentrations over time for four experiments a) *C.debilis*^{sen} at 15°C (6.96 µM Si d⁻¹ and 0.97 µM Si d⁻¹ as two-stage dissolution day 1-20 and day 20-46, or 3.76 µM Si d⁻¹ averaged over 46 days), b) *C.debilis*^{sen} at 5°C (1.32 µM Si d⁻¹, 113 days), c) *C.debilis*^{exp} at 5°C (0.97 µM Si d⁻¹ over 77 days), d) *F.kerguelensis* at 5°C (0.55 µM Si d⁻¹, 123 days). Where dashed lines indicate the assumed linear relationships for the time intervals used to determine dissolution rates, calculated when dissolution began to when concentrations appear too level off.

Physiological state

• Physiological state of diatom cells controls viability and thus dissolution⁶, since it is understood that bacteria are thought to act mostly on detrital diatoms and are unable to remove the organic protective layer whilst cells remain viable/alive.

• Aggregated *C.debilis*^{exp} (●) formed using exponentially growing cells (Fig.5), had a lag period of ~ 11 days in their dissolution when compared to aggregated *C.debilis*^{sen} (■) formed using senescent cells (both at 5°C) (Fig.3d & 3b), likely due to a large fraction of cells remaining alive/viable in this initial period.

• Figure 2 shows the similarity between the rates of dissolution for the senescent and exponential experiments when the lag period of the latter is taken into account (■ 1.32 µM Si d⁻¹ over 113 days, versus ● 0.97 µM Si d⁻¹ over 77 days). The difference may be due to a prolonging of cell viability in the exponential treatment⁶.

• If we assume that the dissolution rate of the *C.debilis*^{exp} (●) experiment would have continued linearly after day 90/end of experiment, ~85% of the total Si pool would have been present as DSi on day 123, which agrees closely with the respective value of the experiment using senescent cells of *C.debilis*^{sen} (■) at the same temperature (81.3%, Fig.3b).

Species comparison

• Despite anticipating a difference, our results were surprising; the rate of dissolution of *F.kerguelensis* (▲) was less than half that of *C.debilis*^{sen} (■) at 5°C (0.55 µM Si d⁻¹ versus 1.32 µM Si d⁻¹, Fig.2).

• Final samples after ~4 months revealed 82.8% of the total Si pool remained in the solid phase (i.e. bSiO₂) for *F.kerguelensis* (▲) (Fig.3a) whereas only 18.7% remained for *C.debilis*^{sen} (■) as most material had dissolved (Fig.3b).

• Dissolution is influenced by differences in diatom geometries, morphologies and structures since these influences the nature of aggregates;

- ▲ *F.kerguelensis* - extremely strong and robust⁷, with elongated cells that form compact chains (Fig.4a) to reduce surface area and result in tightly pack, dense aggregates that we observe to be resilient to dissolution.
- ■ *C.debilis* cells are lightly silicified and spiny (Fig.4b), forming loose chains that transform into 'fluffy' aggregates that are more exposed to dissolution.

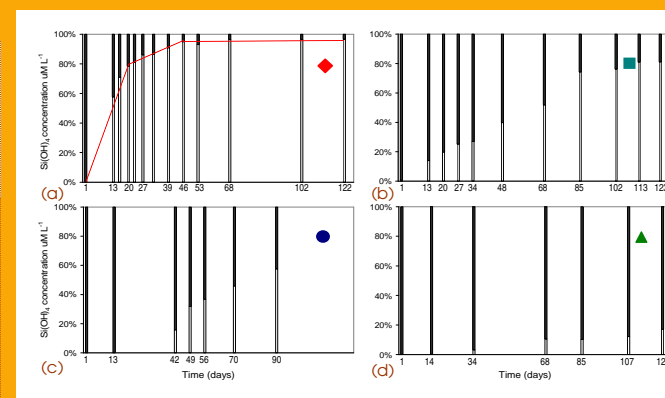


Figure 3 a-c Percentage contribution of DSi and bSiO₂ to total silica pool (DSi+bSiO₂ as Si(OH)₄ µM l⁻¹) for a) for aggregated *C.debilis* cells (initially senescent) rolling in tanks at 15°C for 122 days (◆) where dashed lines approximates 3 phases of dissolution; b) aggregated *C.debilis* cells (initially senescent) rolling in tanks at 5°C for 123 days (■); c) aggregated *C.debilis* cells (initially growing exponentially) rolling in tanks at 5°C for 90 days (●); d) aggregated *F.kerguelensis* cells (initially senescent) rolling in tanks at 5°C for 123 days (▲). Open bars represent percentage DSi and shaded bars bSiO₂.



Acknowledgements: This work was supported by a UK NERC PhD studentship (NER/S/A/2004/12249) through UEA, and the Alfred-Wegener-Institut, Germany.

References

1. Timmermans, K. R., van der Waag, B., and de Baar, H. J. W. 2004. Growth rates, half-saturation constants, and silicate, nitrate, and phosphate depletion in relation to iron availability of four large, open-ocean diatoms from the Southern Ocean. *Limnology and Oceanography* 49 (6), p.p. 2141 - 2151.
2. Verity, P. G., and Smetacek, V. 1995. Organism life cycles, predation, and the structure of marine pelagic ecosystems. *Marine Ecology Progress Series* 130, p.p. 277 - 293.
3. DeMaster, D. J. 1981. The supply and accumulation of silica in the marine environment. *Geochimica et Cosmochimica Acta* 45, p.p. 1715 - 1732.
4. Lewin, J. C. 1961. The dissolution of silica from diatom walls. *Geochimica et Cosmochimica Acta* 21, p.p. 182 - 195.
5. Kamatani, A. 1982. Dissolution rates of silica from diatoms decomposing at various temperatures. *Marine Biology* 68, pp. 91 - 95.
6. Moricau, B., Garvey, M., Raqueneau, O., and Passow, U. 2006. Evidence for reduced biogenic silica dissolution rates in diatom aggregates. *Marine Ecology Progress Series*.
7. Hamm, C. E., Merkel, R., Springer, O., Jurkovic, P., Maier, C., Prechtel, K., and Smetacek, V. 2003. Architecture and material properties of diatom shells provide effective mechanical protection against grazing. *Nature* 421, p.p. 841 - 845.